Integer quantum Hall effect in isotropic three-dimensional crystals

M. Koshino and H. Aoki
Department of Physics, University of Tokyo, Hongo, Tokyo 113-0033, Japan
(Received 23 October 2002; revised manuscript received 14 January 2003; published 30 May 2003)

We show that a series of energy gaps as in Hofstadter's butterfly, which have been shown to exist by Koshino *et al.* [Phys. Rev. Lett. **86**, 1062 (2001)] for *anisotropic* three-dimensional periodic systems in magnetic fields **B**, also arise in the *isotropic* case unless **B** points in high-symmetry crystallographic directions. Accompanying integer quantum Hall conductivities $(\sigma_{xy},\sigma_{yz},\sigma_{zx})$ can, surprisingly, take values $\propto(1,0,0),(0,1,0),(0,0,1)$ even for a fixed direction of **B** unlike in the anisotropic case. We also propose here to intuitively explain the spectra and the quantization of the Hall conductivity in terms of the quantum-mechanical *hopping* between semiclassical orbits in the momentum space, which is usually ignored for weak magnetic fields.

DOI: 10.1103/PhysRevB.67.195336 PACS number(s): 73.43.−f, 72.20.My

I. INTRODUCTION

Appearance of energy gaps in three-dimensional (3D) systems is a hallmark of quantum mechanics in crystals. There, a periodicity, be it atomic or density-wave formation from some mechanism, gives rise to a Bragg's reflection accompanied by energy gaps as Bloch's theorem dictates. Apart from this, there are few occurrences of energy gaps in 3D (unless, of course, nonperturbative, many-body states such as the BCS state are involved).

In 2D systems, by contrast, we do have a remarkable realization of gaps when a magnetic field is applied. For a free 2D electron gas the spectrum even coalesces into a series of sharp Landau levels. When the 2D system has some periodicity (thought of as arising from a periodic potential or tight-binding array of atoms), application of a magnetic field gives rise to a fractal energy gap, which is called ''Hofstadter's butterfly.''[1] One way to understand why the butterfly appears is that the two quantizations, one being Bloch's band structure and the other the Landau quantization, interfere with each other. The interference should occur when the band gap, $\hbar^2/(ma^2)$ (m is electron mass, a is lattice constant), and the cyclotron energy $\hbar\omega_c$ are similar, which indeed amounts to the condition for the appearance of the butterfly, $\phi\sim\phi_0$, where ϕ is the magnetic flux penetrating a unit cell and $\phi_0=h/e$ is the flux quantum.

Once we have an energy gap in a 2D system it is known that the integer quantum Hall effect (IQHE) should occur. Thouless *et al.*[2] in fact have derived a general formula for the quantized Hall conductance in 2D periodic systems without any assumption on the detail of the periodic potential, and have shown that the Hall conductance can be written in terms of some topological invariants.

A natural question is whether we can extend such arguments to 3D systems. Avron *et al.*[3] showed that the topological invariants found by Thouless *et al.* apply not only to the two-dimensional case, but also to any dimensions including 3D. Several authors[4–7] have specifically shown that, *if* an energy gap exists in a 3D Bloch system, it should accompany an IQHE where each component of the Hall tensor σ_{ij} is quantized as a topological invariant. A big question, then, is whether and how gaps can appear in 3D. We have previously shown that the butterflylike spectrum indeed appears in *anisotropic* 3D (quasi-1D) lattices and have derived the quantized Hall tensor for each gap.[8] For the anisotropic case we can intuitively understand this in terms of a mapping between the 3D case and a 2D case. For the *isotropic* case, however, it should seem difficult to have the energy gaps since the magnetic subbands are likely to be overlapped by the dispersion due to the motion along the magnetic field. Several authors[9,10] have computed the energy spectra of the isotropic 3D tight-binding system in magnetic fields (pointing to high-symmetry crystallographic directions), and Kunszt[10] concluded that there are in general no energy gaps although the possibility of gaps cannot be excluded. So the existence of gaps and IQHE has remained an open question.

In this paper, we show that we do have energy gaps in isotropic 3D lattices rather universally, in that all we have to have is a sufficiently large magnetic field **B** pointing to *general directions* (i.e., off the high-symmetry axes). We first show this by calculating energy spectra for various directions of **B**. We have also calculated the Hall tensors, $(\sigma_{xy},\sigma_{yz},\sigma_{zx})$, when the Fermi energy is in each energy gap. They turn out to have values, e.g., $(1,0,0),(0,1,0),(0,0,1)$ in an appropriate unit, even for a fixed direction of **B**, which is surprising and unlike in the anisotropic case. We intuitively explain the energy spectra and the quantization of the Hall conductivity in terms of the quantum-mechanical hopping between semiclassical orbits in the 3D momentum space.

II. FORMULATION OF 3D BLOCH ELECTRONS IN MAGNETIC FIELDS

We take a noninteracting tight-binding model in a uniform magnetic field $\mathbf{B}=(B_x,B_y,B_z)$ pointing to an arbitrary direction. Schrödinger's equation is $-\Sigma_j t_{ij}e^{i\theta_{ij}}\psi_j=E\psi_i$, where ψ_i is the wave function at site i, the summation is over nearest-neighbor sites, and $\theta_{ij}=-e/\hbar\int_j^i\mathbf{A}\cdot d\mathbf{l}$ is the Peierls phase with **A** being the vector potential, $\nabla\times\mathbf{A}=\mathbf{B}$. We consider a simple-cubic lattice with a lattice constant a. Following Kunszt and Zee,[10] we take a gauge $\mathbf{A}=(B_x y-B_y x)(0,-B_z/B_y,1)$, where z is cyclic. Schrödinger's equation then becomes

$$-t_x(\psi_{l-1,m,n}+\psi_{l+1,m,n})-t_y\{e^{-2\pi i\phi_z[l-(\phi_x/\phi_y)(m-1/2)]}\times\psi_{l,m-1,n}+e^{2\pi i\phi_z[l-(\phi_x/\phi_y)(m+1/2)]}\psi_{l,m+1,n}\}-t_z\{e^{-2\pi i(\phi_x m-\phi_y l)}\psi_{l,m,n-1}+e^{2\pi i(\phi_x m-\phi_y l)}\psi_{l,m,n+1}\}=E\psi_{l,m,n}, \quad (1)$$

where (l,m,n) and (t_x,t_y,t_z) are the site indices and the hopping parameters along x,y,z, respectively, and $\phi_i=B_i a^2/\phi_0$ with $\phi_0\equiv h/e$ is respective number of flux quanta penetrating the facet of the unit cell normal to $\hat{\mathbf{e}}_i$. Here we consider rational fluxes,

$$(\phi_x,\phi_y,\phi_z)=\Phi\times(n_x,n_y,n_z), \quad \Phi=P/Q \quad (2)$$

with P,Q being integers and n_i's are mutually prime integers. If we introduce new lattice indices $j=n_x l-n_y m$, the phase factors [exponents in Eq. (1)] become dependent on j alone, so we can write $\psi_{jmn}=e^{i\lambda_2 m+i\lambda_3 n}G_j$, where G_j's are determined by a one-dimensional equation,

$$-t_x(G_{j+n_y}+G_{j-n_y})-t_y\left\{\exp\left(-i\left[2\pi\frac{P}{Q}\frac{n_z}{n_y}\left(j+\frac{n_x}{2}\right)+\lambda_2\right]\right)\times G_{j+n_x}+\exp\left(i\left[2\pi\frac{P}{Q}\frac{n_z}{n_y}\left(j-\frac{n_x}{2}\right)+\lambda_2\right]\right)G_{j-n_x}\right\}-2t_z\cos\left(2\pi\frac{P}{Q}j-\lambda_3\right)G_j=EG_j. \quad (3)$$

While we have a doubly periodic equation in 2D, the reduced equation for 3D is triply periodic in j, where three periodicities come from

$$\exp\left\{-i\left[2\pi\frac{P}{Q}\frac{n_z}{n_y}\left(j+\frac{n_x}{2}\right)+\lambda_2\right]\right\}, \quad \cos\left(2\pi\frac{P}{Q}j-\lambda_3\right),$$

and the discreteness of j. Since the equation has a common periodicity n_yQ, we can apply the Bloch-Floquet theorem to have $G_{j+n_yQ}=e^{i\lambda_1 n_y Q}G_j$, and the Hamiltonian is reduced to an $n_yQ\times n_yQ$ matrix.

III. ENERGY SPECTRA AND HALL CONDUCTIVITIES

Our aim is to search systematically for gapful spectra for the isotropic case and to determine the Hall conductivities for each energy gap. We take a simple-cubic tight-binding lattice with isotropic hopping parameters $t_x=t_y=t_z\equiv t$ and a lattice constant a. We have numerically solved Eq. (3) and obtained the energy spectra versus Φ. Figure 1 shows the result for several field directions: $(n_x,n_y,n_z)=(1,2,3),(1,1,2),(1,1,1)$, and $(0,1,2)$, to represent typical crystallographic directions of **B**.

We can immediately see that a series of gaps appear for $(n_x,n_y,n_z)=(1,2,3)$, while otherwise we have at most solitary gaps. From such results we have found that the spectrum has a series of gaps when no two n_i's coincide and every $n_i\neq 0$; namely, the gapful spectrum arises when **B** *points to general directions* (i.e., off high-symmetry crystallographic axes), although the gaps obviously shrink when $|B|$ is too small ($Ba^2/\phi_0\ll 1$). Unlike anisotropic cases, even in the gapful case as for $(n_x,n_y,n_z)=(1,2,3)$, the subbands tend to overlap with each other so that only the main gaps remain.

While we shall discuss the physical origin of the gaps later, let us first look at the quantum Hall effect. As mentioned, E_F in an energy gap dictates[4–6] quantized Hall conductivities,

$$(\sigma_{yz},\sigma_{zx},\sigma_{xy})=-\frac{e^2}{ha}(m_x,m_y,m_z), \quad (4)$$

where the integer m_i's satisfy a Diophantine equation,

$$\nu=m_x\phi_x+m_y\phi_y+m_z\phi_z+s. \quad (5)$$

Here s is another integer, while ν is the filling factor for the tight-binding band, i.e., the ratio of the number of states below the gap to the total number of states in the whole band. m_i's assigned to each gap are topological invariants, i.e., they never change when external parameters (magnetic field, transfer energies, etc.) are changed continuously as long as the gap remains.

We determine the Hall integers $\mathbf{m}\equiv(m_x,m_y,m_z)$ by tracing ν as a linear function of $\mathbf{\Phi}\equiv(\phi_x,\phi_y,\phi_z)$. In Fig. 1, we can readily estimate ν $(0\leqslant\nu\leqslant 1)$ for each of gaps by counting the number of subbands below the gap, (e.g., if there are two subbands below E_F out of five in total, $\nu=2/5$) and the gradient $d\nu/d\mathbf{\Phi}$ for each gap gives **m**. We can determine m_x,m_y,m_z by scanning the direction of **B** (keeping track of the gap in question), which is exactly how we have obtained the Hall integers here.

The result for (m_x,m_y,m_z) is shown as triple integers in Fig. 1. We can see that the largest series of gaps has $(m_x,m_y,m_z)=(\pm 1,0,0),(0,\pm 1,0)$, or $(0,0,\pm 1)$, which may look indicative of the 2D IQHE since only one of the Hall components is nonzero. However, the direction of the Hall current $\mathbf{j}\propto\mathbf{m}\times\mathbf{E}$ changes even for a fixed **B** as we increase the number of occupied states. This means that the Hall current contributed by *each subband* can have various directions in the 3D space [for instance, the contribution from the band between the gap having $\mathbf{m}=(1,0,0)$ and another having $(0,1,0)$ is $\mathbf{j}\propto(-1,1,0)\times\mathbf{E}$]. Hence we conclude that this is indeed a *3D-specific quantum Hall effect*.

When at least two n_i's coincide as in $(n_x,n_y,n_z)=(1,1,2)$ [Fig. 1(b)] and $(1,1,1)$ [Fig. 1(c)] or one $n_i=0$ as in $(0,1,2)$ [Fig. 1(d)], only solitary gaps or zero gaps (marked with dashed lines) appear. The zero gaps for $(1,1,2)$ and $(1,1,1)$ are associated with the band touching at a Bloch number $(\lambda_1,\lambda_2,\lambda_3)$ in Eq. (3), as first suggested by Hasegawa[9] for the case of $(1,1,1)$. A detailed calculation shows that the dispersion around the band touching is indeed linear in λ's, which is analogous to a zero-mass Dirac particle. The reason for the band touching in 3D can be accounted for as follows. For $(n_x,n_y,n_z)=(1,1,2)$, the gap for $(m_x,m_y,m_z)=(m,0,0)$ and that for $(0,m,0)$ appear along the same line in the E-Φ diagram (Fig. 1), since the problem is

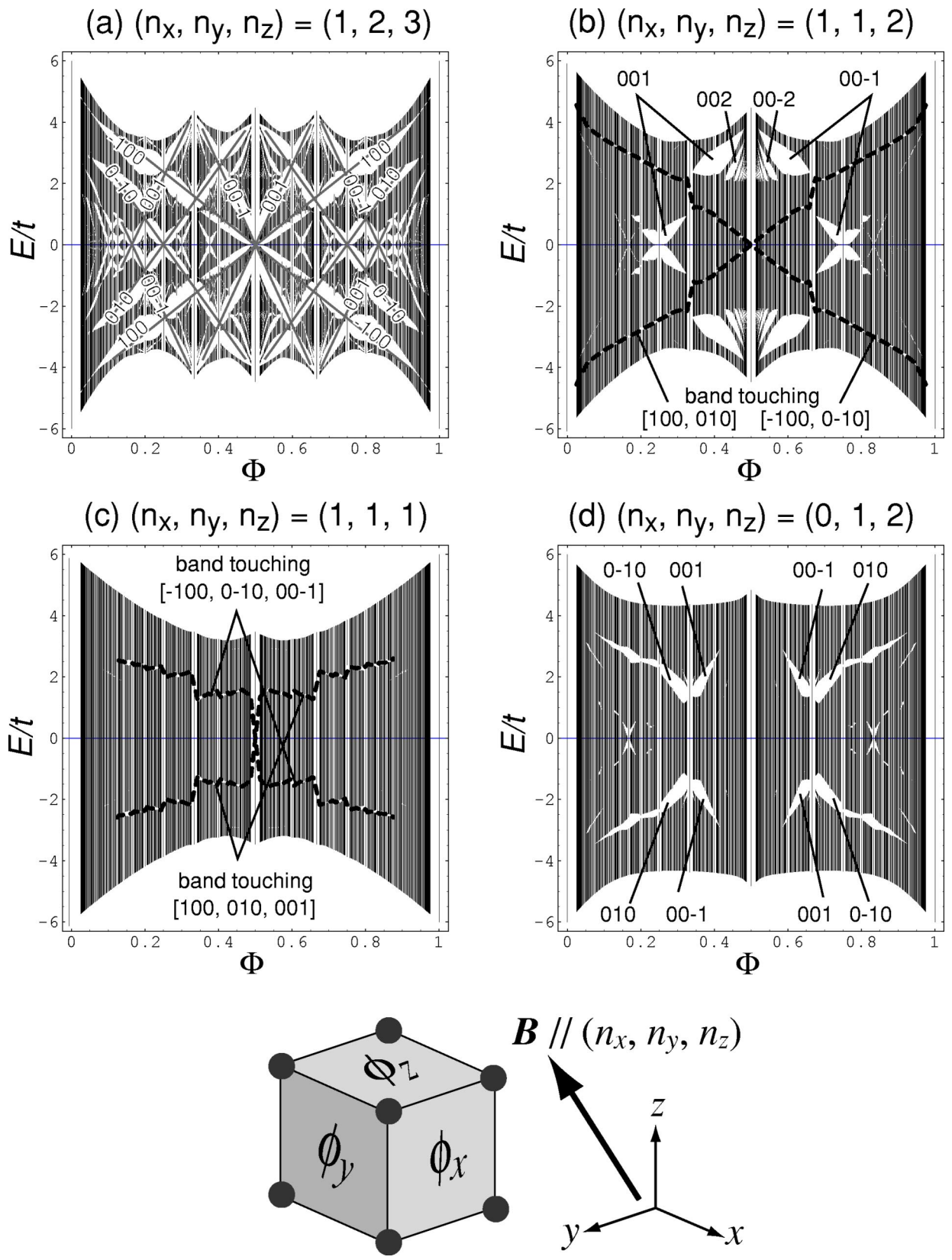

FIG. 1. Energy spectra for the isotropic simple-cubic lattice in the magnetic flux $(\phi_x, \phi_y, \phi_z) = \Phi \times (n_x, n_y, n_z)$. Each spectrum is plotted against Φ with the direction of **B** fixed at (a) $(n_x, n_y, n_z) = (1,2,3)$, (b) (1,1,2), (c) (1,1,1), (d) (0,1,2). Triple integers represent the Hall integers $(\sigma_{xy}, \sigma_{yz}, \sigma_{zx})$ in units of $(-e^2/ha)$. Dashed lines in (b),(c) delineate the zero gap.

symmetric against $x \leftrightarrow y$. If there were no band touching, the Hall integers would become indefinite, which contradicts with the topological argument that we can always uniquely determine m_i's when the gap is finite. So we can conclude that the band touching always occurs when two n_i's coincide, which explains why the series of gaps in case (a) disappears as we make $n_x = n_y$ (b) and further $n_x = n_y = n_z$ in (c). The band touching also occurs in 2D when q in the flux $\phi = p/q$ penetrating the 2D unit cell is even,[11,12] but this is distinct from the present case, since what matters here is the direction of the magnetic field. In addition to the band touching, the energy gaps disappear simply due to the overlapping between subbands as in the case (d) with one of n_i's being zero. The problem of why the band overlapping occurs extensively in (d), but not in (a), will be addressed from a different viewpoint in the following section.

IV. THE MOMENTUM SPACE PICTURE

Electrons in weak magnetic fields are usually described in the momentum space. A textbook example is the semiclassical picture, where an electron is treated as a classical particle driven in the momentum space by a weak magnetic field. As **B** becomes stronger, the semiclassical orbits begin to be mixed and the picture breaks down. Actually this quantum mixing plays a critical role in opening the gaps and in the quantization of the Hall conductivity in 3D, as we show here.

A. 2D momentum space picture

We start with the momentum space picture for 2D for heuristic purposes. Consider the quantum mechanics for a 2D Bloch electron with the dispersion $\varepsilon(p_x, p_y)$ in a magnetic field **B**. If we define the dynamical wavevector $\mathbf{\Pi} \equiv \mathbf{p} + e\mathbf{A}$, the Hamiltonian is written as

$$H = \varepsilon(\Pi_x, \Pi_y),$$

$$[\Pi_x, \Pi_y] = -i\hbar eB. \tag{6}$$

This is an exact quantum equation except that we take the one-band tight-binding approximation (i.e., we have neglected the inter-Bloch-band mixing due to the magnetic field), which is allowed when the periodic potential is strong enough (or the magnetic field is weak enough). The equation in the limit $\hbar eB \to 0$ reduces to the classical Hamilton equation,

$$\dot{\mathbf{\Pi}} = -e \frac{\partial \varepsilon}{\partial \mathbf{\Pi}} \times \mathbf{B}. \tag{7}$$

This means that an electron in (Π_x, Π_y) space moves along a contour of ε. By imposing Bohr-Sommerfeld's quantization condition for a closed orbit, we have

$$\oint \mathbf{\Pi} \times d\mathbf{\Pi} = nheB, \tag{8}$$

with an integer n. The set of Eqs. (7) and (8) is the *semiclassical* approximation, where a closed orbit is identified as one quantum state. This should be distinguished from the full quantum equation (6), in that the quantum fluctuation, which causes the quantum mixing of different semiclassical orbits, is not taken into account.

Here we instead propose a fully quantum-mechanical treatment for Eq. (6), which directly gives, for the first time to the best of our knowledge, Harper's equation.[13] From the commutation relation between Π_x and Π_y, we can express Π_x as a derivative in Π_y, namely, $\Pi_x = -i\hbar eB(\partial/\partial \Pi_y)$, just as $p = -i\hbar \partial/\partial x$ with $[x,p] = i\hbar$ for the canonically conjugate (x,p). Schrödinger's equation in the "Π_y representation" becomes

$$\varepsilon\left(-i\hbar eB \frac{\partial}{\partial \Pi_y}, \Pi_y\right) \Psi(\Pi_y) = E\Psi(\Pi_y), \tag{9}$$

which is the equation to be solved. If we take the dispersion for the 2D tight-binding model with nearest-neighbor hopping,

$$\varepsilon(p_x, p_y) = -2t_x \cos(ap_x/\hbar) - 2t_y \cos(ap_y/\hbar), \tag{10}$$

Eq. (9) becomes

$$-t_x[\Psi(\Pi_y - eBa) + \Psi(\Pi_y + eBa)] - 2t_y \cos(a\Pi_y/\hbar)\Psi(\Pi_y) = E\Psi(\Pi_y), \tag{11}$$

since $\cos A = \frac{1}{2}(e^{iA} + e^{-iA})$ acts as a shift operator when $A \propto \partial/\partial \Pi$. This equation is indeed equivalent to Harper's equation.[13]

B. 3D momentum space picture

Now let us apply the above formulation to 3D systems. We take a Bloch electron with the dispersion $\varepsilon(p_x, p_y, p_z)$ in a magnetic field $\mathbf{B} = (B_x, B_y, B_z)$. Let us again denote the direction of **B** as $\mathbf{n} \equiv (n_x, n_y, n_z)$ whose components will be assigned a set of integers. We set a new frame (x', y', z') in which the magnetic field point to $(0,0,1)$. If we take the vector potential **A** with $A_{z'} = 0$, we have

$$H = \varepsilon(\Pi_{x'}, \Pi_{y'}, p_{z'}), \tag{12}$$

where $\Pi_i = p_i + eA_i$ $(i = x', y')$ with $[\Pi_{x'}, \Pi_{y'}] = -i\hbar eB$ while $p_{z'}$ remains a quantum number. Here we take a cubic dispersion,

$$\varepsilon(p_x, p_y, p_z) = -2t_x \cos(ap_x/\hbar) - 2t_y \cos(ap_y/\hbar) - 2t_z \cos(ap_z/\hbar). \tag{13}$$

Equation (12) is then written in the new frame as

$$\varepsilon(\Pi_{x'}, \Pi_{y'}, p_{z'}) = -2t_x \cos[\mathbf{c}_x \cdot \mathbf{\Pi}_\perp/\hbar + (n_x/|\mathbf{n}|)ap_{z'}/\hbar] - 2t_y \cos[\mathbf{c}_y \cdot \mathbf{\Pi}_\perp/\hbar + (n_y/|\mathbf{n}|)ap_{z'}/\hbar] - 2t_z \cos[\mathbf{c}_z \cdot \mathbf{\Pi}_\perp/\hbar + (n_z/|\mathbf{n}|)ap_{z'}/\hbar], \tag{14}$$

where $\mathbf{\Pi}_\perp \equiv (\Pi_{x'}, \Pi_{y'})$ and

$$\mathbf{c}_x = \tilde{a}(n_z n_x/|\mathbf{n}|, -n_y),$$

$$\mathbf{c}_y = \tilde{a}(n_y n_z/|\mathbf{n}|, n_x),$$

$$\mathbf{c}_z = \tilde{a}(-(n_x^2+n_y^2)/|\mathbf{n}|, 0), \tag{15}$$

with $\tilde{a} \equiv a/(n_x^2+n_y^2)^{1/2}$. Now we can see that our 3D problem is reduced to a 2D problem having three periods [while the Hofstadter problem (2D Bloch system in B) is reduced to a 1D system having two periods].

If, following the above formulation, we now put $\Pi_{y'} = i\hbar eB\partial/\partial\Pi_{x'}$, Schrödinger's equation in the $\Pi_{x'}$ representation becomes, after some algebra,

$$\begin{aligned} -t_x\Bigg[&\exp\left\{ 2\pi i\Phi\tilde{n}_z\tilde{n}_x\left(j+\frac{n_y}{2}\right) + i\frac{n_x}{|\mathbf{n}|}\frac{ap_{z'}}{\hbar}\right\}\Psi_{j+n_y} \\ &+ \exp\left\{ -2\pi i\Phi\tilde{n}_z\tilde{n}_x\left(j-\frac{n_y}{2}\right) - i\frac{n_x}{|\mathbf{n}|}\frac{ap_{z'}}{\hbar}\right\}\Psi_{j-n_y}\Bigg] \\ -t_y\Bigg[&\exp\left\{ 2\pi i\Phi\tilde{n}_y\tilde{n}_z\left(j-\frac{n_x}{2}\right) + i\frac{n_y}{|\mathbf{n}|}\frac{ap_{z'}}{\hbar}\right\}\Psi_{j-n_x} \\ &+ \exp\left\{ -2\pi i\Phi\tilde{n}_y\tilde{n}_z\left(j+\frac{n_x}{2}\right) - i\frac{n_y}{|\mathbf{n}|}\frac{ap_{z'}}{\hbar}\right\}\Psi_{j+n_x}\Bigg] \\ -2t_z &\cos\left(2\pi\Phi j + \frac{n_z}{|\mathbf{n}|}\frac{ap_{z'}}{\hbar}\right)\Psi_j = E\Psi_j, \end{aligned} \tag{16}$$

where $j \equiv (1/eB\tilde{a})\Pi_{x'}$, $\tilde{n}_i \equiv n_i/(n_x^2+n_y^2)^{1/2}$, and Φ is defined as before as $(\phi_x,\phi_y,\phi_z) = \Phi\mathbf{n}$. We can show that this equation is equivalent to Eq. (3) through a certain phase transformation, as it should.

This momentum picture enables us to see how the total spectrum comes from dispersion relations versus $p_{z'}$, which eventually helps in intuitively understanding how the energy gaps open and how the Hall conductivities are quantized. We examine the situation where the gaps begin to open in the quantum regime as approached from the semiclassical side.

Let us first look at how the energy spectra can have gaps for general directions of $\mathbf{n}$ [$\propto(1,2,3)$ in Fig. 2]. We show in Fig. 2 the band structure versus $p_{z'}$ in Eq. (16), along with contour plots of the dispersion $\varepsilon(\Pi_{x'},\Pi_{y'},p_{z'})$ [Eq. (14)], for various values of $p_{z'}$. ε accommodates closed orbits around its peaks and dips in the semiclassical picture, where the area enclosed by each orbit must be a multiple of heB. So the different wells have different sets of discrete levels, and each level moves on the energy axis as $p_{z'}$ is changed since ε changes its form with $p_{z'}$. When the levels belonging to different wells in $(\Pi_{x'},\Pi_{y'})$ space coincide, the states will strongly resonate quantum mechanically and an energy gap will arise. In Fig. 2 we show the case where the gaps begin to open with $(\phi_x,\phi_y,\phi_z) = (1/8)(1,2,3)$, for which the strong mixing of orbits is seen to result in significant level repulsions. We attach for comparison the result for an almost semiclassical case when the magnetic field, $(\phi_x,\phi_y,\phi_z) = (1/45)(1,2,3)$, is so small that the mixing is weak and the level repulsion is almost negligible.

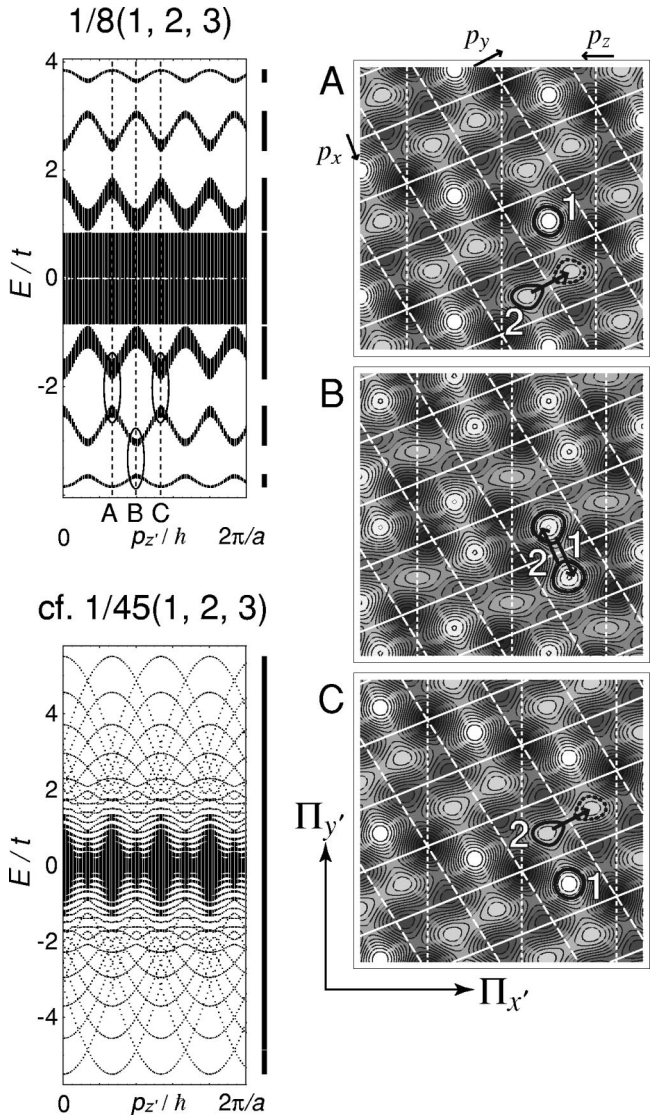

FIG. 2. Left: Energy spectra versus $p_{z'}$ for Eq. (16) $(\phi_x,\phi_y,\phi_z) = (1/8)(1,2,3)$ [along with a weak field case of $(1/45)(1,2,3)$ for comparison]. The final band structure is indicated as bars at the right-hand edge of each spectrum. The energy spectra are periodic in $p_{z'}$ with period $2\pi\hbar/(a|\mathbf{n}|)$ with $\mathbf{n}=(1,2,3)$ here. The values of p_z labeled as A,B,C correspond to the plots on the right panel. Right: Gray scale plot (with lighter areas corresponding to dips) of the dispersion $\varepsilon(\Pi_{x'},\Pi_{y'},p_{z'})$ [Eq. (14)] versus $(\Pi_{x'},\Pi_{y'})$ for $\mathbf{n}=(1,2,3)$, for various values of $p_{z'}$ (labeled A,B,C on the left panel). Three sets of white lines represent the intersections of the boundaries of the reciprocal unit cells normal to p_x,p_y,p_z, respectively. These lines also move as $p_{z'}$ is changed, since the zone faces are oblique with $z' \| \mathbf{B}$. Motion of the orbits with $p_{z'}$ for the lowest and the second subbands are indicated as 1 and 2, respectively, where the jumps to adjacent orbits are represented as arrows and the resulting energy gaps encircled on the left panel.

In terms of the semiclassical orbits, the change in $p_{z'}$ causes the orbits to hop to adjacent positions at every resonance. A virtue of this picture is that *the distance and the direction of the hopping exactly indicates the Hall integers*, as shown in the following. If we apply an infinitesimal elec-

tric field **E** to the system, $p_{z'}$ is dragged adiabatically according to an equation, $dp_{z'}/dt=-eE_{z'}$, where $E_{z'}$ is the component along z'. After $p_{z'}$ is changed by $\delta p_{z'}/\hbar \equiv 2\pi/(a|\mathbf{n}|)$ (the period with which the spectrum repeats itself), every state must come back to an equivalent position in the reciprocal unit cell. The increment in the momentum space, $\delta\mathbf{\Pi}=(\delta\Pi_{x'},\delta\Pi_{y'},\delta p_{z'})$, with which the orbit is shifted over the one period satisfies

$$\frac{\delta\mathbf{\Pi}}{\hbar}=\mp\frac{2\pi}{a}\delta\mathbf{m},$$

$$\delta\mathbf{m}=\delta m_x\hat{\mathbf{e}}_x+\delta m_y\hat{\mathbf{e}}_y+\delta m_z\hat{\mathbf{e}}_z, \tag{17}$$

where $\mp$ corresponds to positive and negative $E_{z'}$, respectively, and δm_i's are integers assigned to each subband. The integers satisfy a relation $\delta\mathbf{m}\cdot\mathbf{n}=1$, since $\delta p_{z'}/\hbar=2\pi/(a|\mathbf{n}|)$.

We can immediately translate $\delta\mathbf{\Pi}$ into the motion in the real space normal to z' using the relationship between the relative coordinate $\boldsymbol{\xi}$ of the cyclotron motion and the dynamical wave vector $\mathbf{\Pi}$,

$$\delta\boldsymbol{\xi}=-\frac{1}{eB}\hat{\mathbf{e}}_{z'}\times\delta\mathbf{\Pi}. \tag{18}$$

Since the system has no dissipation as long as E_F is in a gap, $\mathbf{E}_{z'}$ should cause no net current along z'. Therefore the velocity averaged over one period in time, $T=\delta p_{z'}/(e|E_{z'}|)$, is $\mathbf{v}=\delta\boldsymbol{\xi}/T=(|\mathbf{n}|/B)\mathbf{E}_{z'}\times\delta\mathbf{m}$. The Hall current due to $\mathbf{E}_{z'}$ is then calculated as

$$\mathbf{j}=-\rho e\mathbf{v}=\frac{e^2}{ha}\delta\mathbf{m}\times\mathbf{E}_{z'}, \tag{19}$$

where $\rho=eB/(ha|\mathbf{n}|)$ is the density of states per subband and per unit volume. From this expression we can write the Hall tensor as $\hat{\boldsymbol{\sigma}}_\perp=-(e^2/ha)\delta\mathbf{m}_\perp$, where we have expressed the Hall conductivities as

$$\sigma_{ij}\equiv\varepsilon_{ijk}\hat{\sigma}_k$$

with the unit antisymmetric tensor ε_{ijk} and $\perp$ represents the component normal to z'. The normal component of the electric field $\mathbf{E}_\perp$, on the other hand, causes a classical drift with the velocity $\mathbf{v}=(\mathbf{E}_\perp\times\mathbf{B})/B^2=(|\mathbf{n}|/B)\mathbf{E}_\perp\times\delta\mathbf{m}$, which immediately leads to $\hat{\sigma}_{z'}=-(e^2/ha)\delta m_{z'}$. Combining these, we end up with a simple formula for the quantized Hall conductivity carried by the corresponding subband,

$$\hat{\boldsymbol{\sigma}}=-\frac{e^2}{ha}\delta\mathbf{m}. \tag{20}$$

We have thus derived the quantization of the 3D Hall conductivity from the momentum space hopping, as an approach alternative to the usual Kubo formula.

The problem of the transport in adiabatically varying potentials (so-called *Thouless pumping*) was first considered by Thouless[14] for the one-dimensional case. He showed that the 2D QHE in periodic potentials may be understood in terms of a fictitious 1D system having two periodic potentials that slide adiabatically with each other. The discussion we have given here to describe the 3D QHE may be regarded as a two-dimensional version of the Thouless pumping.

We can actually identify the Hall integers δm_i for each subband by keeping track of the motion of the orbits with $p_{z'}$. Figure 2 typically depicts how a state in the first band moves by (1,0,0), by which we mean the state jumps once across a reciprocal cell boundary normal to p_x (whose intersection is shown as one of the white lines) but not across p_y or p_z. The state in the second band moves by $(-1,1,0)$. These triple numbers are the very Hall integers, $(\delta m_x,\delta m_y,\delta m_z)$, carried by each subband [not to be confused with the total Hall integer, (m_x,m_y,m_z) as we remarked above], and are in accordance with the result in Fig. 1(a).

We can now comment on the relation with the usual treatment of 3D QHE.[4–6] By summing up $\delta\mathbf{m}\cdot\mathbf{n}=1$ over the occupied subbands, we have $\mathbf{m}\cdot\mathbf{n}=r$, where r is the number of occupied subbands and $\mathbf{m}$ is the summation of $\delta\mathbf{m}$ over them. Since r is related to the filling of the tight-binding band as $\nu=r\times\rho/(1/a^3)$, we obtain

$$\nu=m_x\phi_x+m_y\phi_y+m_z\phi_z, \tag{21}$$

which coincides with the Diophantine equation (5) with $s=0$. While the discussion here is for the lower half of the tight-binding band, we can make a similar argument for the upper half in terms of hole orbits, which in turn corresponds to $s=1$. So in our picture above, only the gaps with $s=0(1)$ are taken into account for the lower (upper) half band, and the rest are neglected. We can actually show that the widths of the neglected gaps are much smaller than those of the main gaps when the magnetic field is weak ($\Phi\ll1$), which is exactly the situation considered here, since we approached the quantum regime from the semiclassical side.

The mapped picture also gives an intuitive explanation why we have so few gaps for the symmetric case $\mathbf{n}\propto(1,1,2)$, (1,1,1) and zero-component case $\mathbf{n}\propto(0,1,2)$ as seen in Fig. 3. When two components in $\mathbf{n}$ coincide as in (1,1,2), two levels can cross (for the value of $p_{z'}$ labeled as B), but a gap does not open because the couplings between semiclassical orbits along p_x and p_y occur symmetrically (in a zigzag fashion), so that the bands do not split. This is exactly the band touching discussed in Sec III. When the symmetry is even higher as in $\mathbf{n}\propto(1,1,1)$, couplings along p_x, p_y, and p_z all become symmetric and the band touching occurs at every crossing. If $\mathbf{n}$ contains a zero component as in (0,1,2), two of the plane waves for ε become parallel and the wells having the same depth become connected along the perpendicular direction. This results in a strong mixing between the states along that trough, so that the minibands for each value of $p_{z'}$ become wider. So, while the energy gaps do arise when the energies of the adjacent troughs coincide, these gaps tend to be overlapped in energy by other wide bands.

The momentum space picture introduced here can be interpreted from another description. In the Appendix, we propose a ''duality,'' a quantum mapping between the momen-

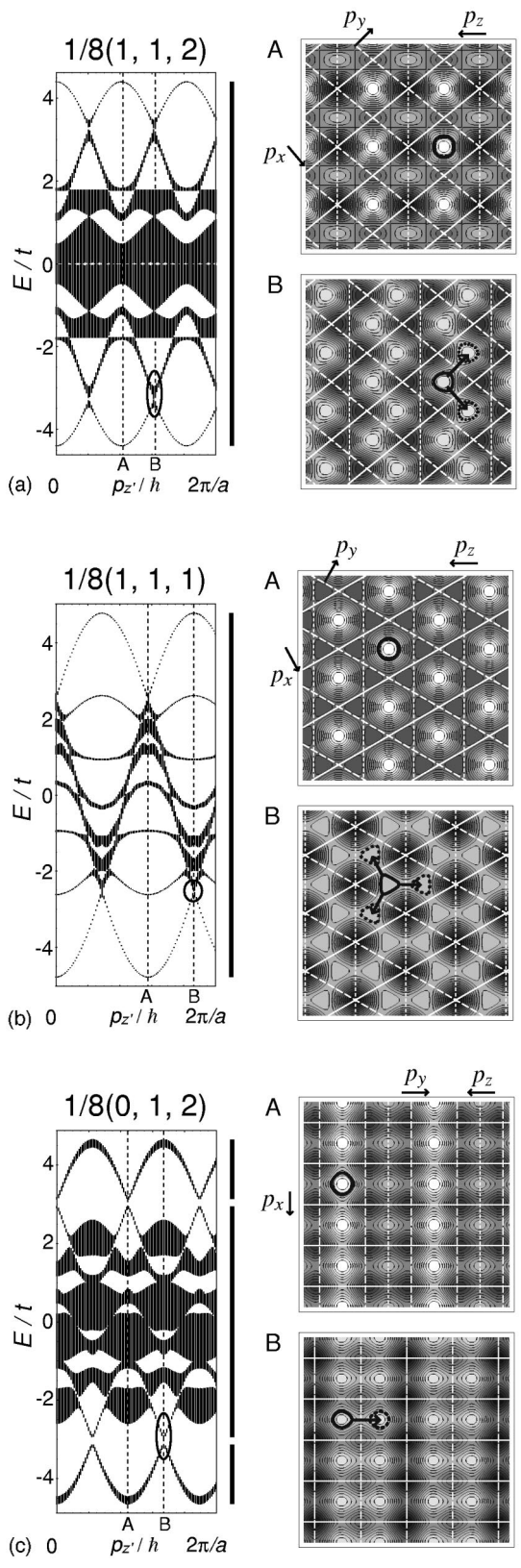

FIG. 3. The plots similar to Fig. 2 for the case of $(\phi_x,\phi_y,\phi_z)=(1/8)(n_x,n_y,n_z)$: $(n_x,n_y,n_z)=(1,1,2)$, $(1,1,1)$, and $(0,1,2)$.

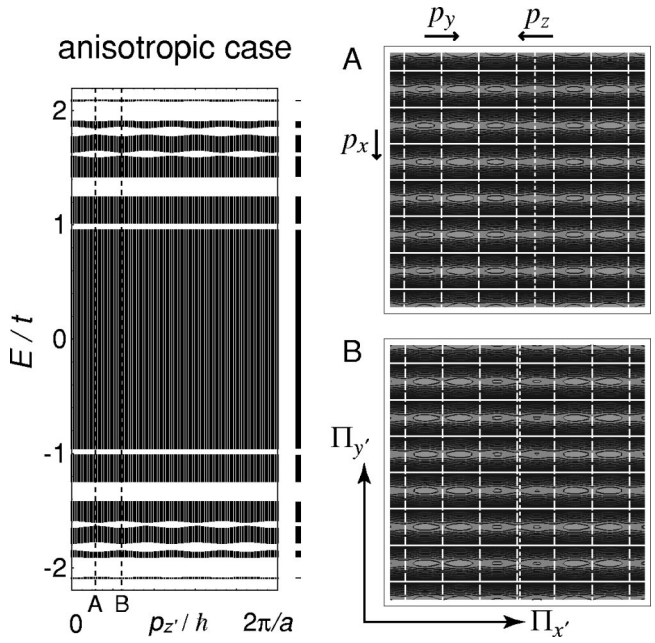

FIG. 4. A plot similar to Fig. 2 for an anisotropic 3D system with $(t_x,t_y,t_z)=(1.0,0.1,0.1)$ for $(\phi_x,\phi_y,\phi_z)=(1/15)(0,1,4)$. The contours highlight the troughs.

tum space description for the weak **B** problem and the real-space picture for the strong **B** case.

In our previous paper[8] we have shown that an analog of Hofstadter's butterfly arises (i) as a function of the *tilting angle* θ in magnetic field tilted in the yz plane (ii) in *anisotropic* $(t_x \gg t_y,t_z)$ 3D lattices. We can reinterpret the physics of the 3D butterfly in terms of the momentum space picture introduced above. In Fig. 4, we show a contour plot of $\varepsilon(\mathbf{p})$ on a cross section along with the energy spectra plotted against $p_{z'}$. We can see that the dominant term associated with t_x gives troughs and ridges, and a small perturbation due to t_y and t_z gives small corrugations to each of them. The semiclassical orbits in the pockets in the corrugation hop onto each other and form a one-dimensional chain. So the system can be regarded as an array of independent chains with two periods $(\propto 1/\phi_y,\propto 1/\phi_z)$, which is just equivalent to a Harper's equation for the 2D Hofstadter's problem.[8] Thus we can understand why the butterfly appears around the top and the bottom of the band.

V. EXPERIMENTAL FEASIBILITY

Let us comment on the magnitude of the magnetic field required to observe the energy gaps in isotropic 3D systems. As mentioned, it is essential for the existence of the energy gaps that the quantum coupling exists between the semiclassical orbits in the different wells. For that, zero-point energy of the bound states in wells should be of the order of the typical depth of the wells. In other words, the typical ''well'' area in the momentum space should be of the order of a quantized area heB. For the isotropic crystals considered

here, this condition leads to $(h/a)^2 \sim heB$ [h/a is the period in $\varepsilon(\mathbf{p})$], which is simply $Ba^2/\phi_0 \sim 1$. The situation is the same as in the 2D Hofstadter problem, so the required field for atomic lattice constants is huge ($B \sim 10^5$ T for $a = 2$ Å). If we consider systems with larger unit cells, as in solid fullerene or zeolites with $a = 10$ Å, the required B is reduced to 10^3 T but is still large. In the anisotropic case discussed in Ref. 8, by contrast, the condition is much less stringent. This is because the typical well area is $(h/a)d$ with d being the typical valley width, so the condition relaxes to $(h/a)d \sim heB$, where B can be made as small as one wishes by increasing the anisotropy (since $t_y, t_z \to 0$ leads to $d \to 0$), although the scale of the energy gap shrinks. So what we have here is a trade-off between large B required with large-energy gaps (isotropic case) and smaller B suffices with small gaps (anisotropic).

Another point is that a real 3D sample has always surfaces. Halperin and the present authors have shown, in general, that the 3D integer QHE should accompany quantized *wrapping* current, whose intensity and direction are dictated by the quantum Hall integers $\hat{\boldsymbol{\sigma}}$.[19] This should apply to the present case of isotropic QHE as well.

VI. CONCLUSION

We have investigated the energy spectra in the isotropic 3D lattice in magnetic fields applied in arbitrary directions, for which we have shown that the energy gaps arise unless the magnetic field points to high-symmetry crystallographic directions. We have also identified the quantum Hall integers for each of gaps. In the latter part of the paper we have examined a momentum space picture and found that the mixing of the different momentum space orbits beyond the semiclassical approximation is essential for the gap formation. This picture further provides a perspective for the quantum Hall effect in 3D, where the Hall current is estimated from the geometry of adiabatic jumps of the orbit.

ACKNOWLEDGMENT

M.K. would like to thank the Japan Society for Promotion of Science for a financial support.

APPENDIX: DUALITY BETWEEN THE MOMENTUM SPACE AND REAL SPACE

We propose here that there exists a duality that relates the momentum space picture (Sec. IV) in a weak magnetic field to the real-space picture in a strong magnetic field, where B translates into $1/B$. Using a quantum-mechanical mapping between the two cases, we are able to discuss the relationship between the energy spectra and the Hall conductivities for the both systems.

We first discuss the duality in 2D and then extend it to 3D. As a counterpart to the momentum space picture (6), we consider another 2D Bloch system in a magnetic field B. The Hamiltonian is written in real space as

$$H = \frac{1}{2m}(\mathbf{p} + e\mathbf{A})^2 + V(\mathbf{r}) = \frac{1}{2m}\boldsymbol{\Pi}^2 + V\left(\mathbf{R} - \frac{1}{eB}\hat{\mathbf{e}}_z \times \boldsymbol{\Pi}\right), \tag{A1}$$

where $V(\mathbf{r})$, with $\mathbf{r} \equiv (x,y)$, is a periodic potential, $\boldsymbol{\Pi} \equiv \mathbf{p} + e\mathbf{A}$, and $\mathbf{R} = \mathbf{r} - \boldsymbol{\xi}$ the cyclotron-motion guiding center with the relative coordinate given as $\boldsymbol{\xi} = -(1/eB)\hat{\mathbf{e}}_z \times \boldsymbol{\Pi}$. When the magnetic field is strong enough (or the potential V is weak enough) so that (i) the magnetic length $l = \sqrt{\hbar/(eB)}$ is much shorter than the length scale over which V varies, and that (ii) the different Landau levels are not mixed, we can consider $\boldsymbol{\Pi}$ to be frozen. More precisely, the kinetic energy [the first term in Eq. (A1)] reduces to a constant from (ii), while the second term can be approximated as $V(\mathbf{R})$ from (i). The Hamiltonian then becomes, up to a constant,

$$H \approx V(X,Y),$$

$$[X,Y] = i\hbar/(eB). \tag{A2}$$

We can see that Eqs. (6) and (A2) are identical if we translate as

$$\boldsymbol{\Pi} \leftrightarrow \mathbf{X}, \quad \varepsilon \leftrightarrow V, \quad \hbar eB \leftrightarrow \frac{\hbar}{eB}. \tag{A3}$$

So we recognize that there exists a duality between the 2D system with a strong periodic potential in a weak B (one band tight-binding model) and the 2D system with a weak periodic potential in a strong field (one Landau level approximation). For the Landau level in the latter case, we expect that the duality holds best in the lowest Landau level, since the wave function is most localized in that level to make Eq. (A2) valid. In the semiclassical sense, the latter picture describes the drifts, the guiding center of the cyclotron motion along equipotential contours in the real space, while the former represents the motion along contours of $\varepsilon(\mathbf{p})$ in the momentum space.

The duality introduced here provides a physical basis for Hofstadter's observation[1] on the mapping between the tight-binding and weak-potential systems[15] for the square lattice, and also generally applicable to any 2D lattices, or, remarkably, 3D cases as well, as we shall see below. Another duality is found by Ishikawa *et al.*,[18] which is distinct from ours, in that one Landau level is mapped to one Landau level in the latter while one Landau level is mapped to one Bloch band in the present case.

Specifically, it is interesting to see how the Hall conductivities are related between them for the corresponding energy gaps. For the 2D case, Thouless *et al.*[2] have shown the relationship between the Hall integers in the tight-binding and in the strong-field limits. Here we first review this in the context of our duality. Diophantine's equation for an energy gap in the 2D tight-binding case [a 2D version of Eq. (5)] is

$$\nu_B = t\phi + s, \tag{A4}$$

where s,t are integers, ν_B is the tight-binding band filling, and ϕ is the number of fluxes penetrating the 2D unit cell. The equation for the corresponding gap in the 2D strong-field case is written with the same s,t as

$$\nu_L = t(1/\phi) + s, \tag{A5}$$

where ν_L is the Landau-level filling factor, i.e., the fraction of the filled states in the lowest Landau level, and ϕ is replaced with $1/\phi$ according to the duality [Eq. (A3)]. From the relation $\nu_L = \nu_B/\phi$, we can translate Eq. (A5) into

$$\nu_B = s\phi + t. \tag{A6}$$

Now we can see that the two topological integers s and t are *interchanged* between the dual [(tight-binding (A4) $\leftrightarrow$ strong-field (A6)] cases. The Widom-Středa formula[16,17]

$$\sigma_{xy} = -\frac{e^2}{h}\frac{\partial \nu_B}{\partial \phi} \tag{A7}$$

then gives $-(e^2/h)t$ in the former case, $-(e^2/h)s$ in the latter.

The duality applies also to the 3D system. If we plug the above discussion to the Hamiltonian (12), we immediately see that the 3D system is mapped to a system in a *fictitious* 2D space $(\Pi_{x'}, \Pi_{y'})$ with a potential $\varepsilon(\Pi_{x'}, \Pi_{y'}, p_{z'})$ in a fictitious magnetic field B^* with $\hbar e B = \hbar/(eB^*)$. The mapping is valid for large B^*, i.e., small B. The fictitious potential is a cross section of the 3D dispersion incised at $p_{z'}$ by a plane perpendicular to **B**. The Hamiltonian for the fictitious 2D system is

$$H = \frac{1}{2m}(\mathbf{p}^* + e\mathbf{A}^*)^2 + \varepsilon(x^*, y^*, p_{z'}), \tag{A8}$$

where $(x^*, y^*) \equiv (\Pi_{x'}, \Pi_{y'})$, $\mathbf{p}^* \equiv -i\hbar(\partial/\partial\Pi_{x'}, \partial/\partial\Pi_{y'})$, and $\mathbf{A}^*$ is a vector potential for the fictitious magnetic field $(0,0,B^*)$. Since we assume a large B^*, the wave function can be expanded within the basis for the lowest Landau level,

$$|k_y^*\rangle = \exp(ik_y^* x^*)\exp\left[-\frac{(x^* + k_y^* l^{*2})^2}{2l^{*2}}\right], \tag{A9}$$

with the fictitious magnetic length $l^* \equiv \sqrt{\hbar/(eB^*)}$. If we take dispersion (14), Schrödinger's equation becomes the same as Eq. (16), except that we have now $j = (\sqrt{n_x^2 + n_y^2}/a)k_y^*$ and the hopping parameters

$$\tilde{t}_i = t_i e^{-c_i^2/(4\hbar e B^*)} \quad (i = x, y, z), \tag{A10}$$

with $c_i \equiv |\mathbf{c}_i|$ defined in Eq. (15). We can see that the equation reduces to Eq. (16) in the strong B^* limit (i.e., weak B limit) as expected.

The relationship in the Hall conductivities with respect to the duality can be readily extended to the 3D case. If we take an energy gap in the 3D system with $(\sigma_{yz}, \sigma_{zx}, \sigma_{xy}) = -e^2/ha(m_x, m_y, m_z)$, the Hall conductivity in the corresponding 2D system becomes $-(e^2/h)s$, where m_i and s are related via Diophantine equation (5).

[1] D.R. Hofstadter, Phys. Rev. B **14**, 2239 (1976).
[2] D.J. Thouless, M. Kohmoto, P. Nightingale, and M. den Nijs, Phys. Rev. Lett. **49**, 405 (1982).
[3] J.E. Avron, R. Seiler, and B. Simon, Phys. Rev. Lett. **51**, 51 (1983).
[4] B.I. Halperin, Jpn. J. Appl. Phys., Suppl. **26**, 1913 (1987).
[5] G. Montambaux and M. Kohmoto, Phys. Rev. B **41**, 11 417 (1990).
[6] M. Kohmoto, B.I. Halperin, and Y. Wu, Phys. Rev. B **45**, 13 488 (1992).
[7] The 3D topological invariants are later interpreted as Berry's phase by J. Goryo and M. Kohmoto, J. Phys. Soc. Jpn. **71**, 1403 (2002).
[8] M. Koshino, H. Aoki, K. Kuroki, S. Kagoshima, and T. Osada, Phys. Rev. Lett. **86**, 1062 (2001); Phys. Rev. B **65**, 045310 (2002).
[9] Y. Hasegawa, J. Phys. Soc. Jpn. **59**, 4384 (1990); **61**, 1657 (1991).
[10] Z. Kunszt and A. Zee, Phys. Rev. B **44**, 6842 (1991).
[11] M. Kohmoto, Phys. Rev. B **39**, 11 943 (1989).
[12] Y. Hatsugai and M. Kohmoto, Phys. Rev. B **42**, 8282 (1990).
[13] P.G. Harper, Proc. Phys. Soc., London, Sect. A **68**, 874 (1955).
[14] D.J. Thouless, Phys. Rev. B **27**, 6083 (1983).
[15] A. Rauh, Phys. Status Solidi B **69**, K9 (1975).
[16] A. Widom, Phys. Lett. **90A**, 474 (1982).
[17] P. Středa, J. Phys. C **15**, L718 (1982).
[18] K. Ishikawa, N. Maeda, T. Ochiai, and H. Suzuki, Phys. Rev. B **58**, 1088 (1998).
[19] M. Koshino, H. Aoki, and B.I. Halperin, Phys. Rev. B **66**, 081301(R) (2002).